A quasi-dimensional model for SI engines fuelled with gasoline-alcohol blends: knock modeling.

Sileghem, L.*[1], Wallner T.[2], Verhelst S.[1]

[1]Department of Flow, Heat and Combustion Mechanics, Ghent University, Sint-Pietersnieuwstraat 41, B-9000 Ghent, Belgium

[2]Argonne National Laboratory, Argonne, IL, USA

*Corresponding author:

Email: Louis.Sileghem@UGent.be

KEYWORDS – Alcohol fuel, Spark Ignition Engine, Thermodynamic, Modeling, Knock

ABSTRACT

As knock is one of the main factors limiting the efficiency of spark-ignition engines, the introduction of alcohol blends could help to mitigate knock concerns due to the elevated knock resistance of these blends. A model that can accurately predict their autoignition behavior would be of great value to engine designers. The current work aims to develop such a model for alcohol-gasoline blends. First, a mixing rule for the autoignition delay time of alcohol-gasoline blends is proposed. Subsequently, this mixing rule is used together with an autoignition delay time correlation of gasoline and an autoignition delay time correlation of methanol in a knock integral model that is implemented in a two-zone engine code. The predictive performance of the resulting model is validated through comparison against experimental measurements on a CFR engine for a range of gasoline-methanol blends.

The knock limited spark advance, the knock intensity, the knock onset crank angle and the value of the knock integral at the experimental knock onset have been simulated and compared to the experimental values derived from in-cylinder pressure measurements.

1. INTRODUCTION

There is a renewed interest in methanol as alternative fuel for internal combustion engines. This has led to fleet trials of both high- and low-level methanol blends in China, Australia and Israel. China has declared coal-based methanol as a strategic transportation fuel to ensure its energy-independence. M85 vehicles have been around for some years, especially in coal-abundant provinces but now methanol is also finding its way into the densely populated coastal regions of China [1]. China's central government has launched a demonstration of light-and heavy-duty vehicles running on M85 (85% methanol and 15% gasoline) and M100 (100% methanol) in the Shanxi and Shaanxi provinces, as well as in the city of Shanghai. In Israel and Australia, fleet trials with low-level methanol blends have also started [1].

Combustion knock is one of the major factors limiting the efficiency of spark ignition engines. It is caused by the autoigniting pockets of unburned gas [2]. The energy release associated with knock is usually very fast. This causes high local pressures and pressure waves across the combustion chamber. These waves can lead to mechanical and thermal damage to the engine. As autoignition is a highly temperature and pressure dependent process, knock is often avoided by retarding spark timing, enriching the mixture, lowering the compression ratio or limiting the charge pressure in boosted engines. These classical measures usually reduce engine performance and efficiency. Alternative solutions may feature a combination of new technologies such as VVT (variable valve timing) or cooled EGR (exhaust gas recirculation) and fuels with elevated anti-knock resistance. In this respect, light alcohols, such as methanol and ethanol, are interesting candidate fuels [3]. Alcohol fuels have a high knock tolerance for a variety of reasons. First and foremost methanol and ethanol have an elevated chemical resistance to autoignition, which is

reflected in their high octane number (ON= 109) [4]. This is due to the single-stage autoignition behavior of alcohols. Compared to two-stage autoignition fuels such as gasoline, they do not exhibit a cool-flame reaction. This reaction takes place at temperatures below 900 K and promotes the main autoignition at high temperature. As autoignition in engines takes place at unburned mixture temperatures of 800-900K, it is the prime reason for the reduced delay time of gasoline compared to alcohols [5]. Additionally the high latent heat of vaporization of light alcohols lowers the temperature of the unburned gas, further reducing the tendency to knock. In directly injected E85 engines the knock inhibiting effect of vaporization cooling has been shown to be comparable to the chemical effect [6]. For PFI (port fuel injected) engines, this effect is more modest. Finally, the increased (laminar) burning velocity of light alcohols helps to suppress knock as more end gas is burned before it can reach autoignition conditions [7, 8].

As there is a renewed interest in alcohols as alternative fuel, an accurate predictive knock model for alcohols fuels would be of great value to engine designers.

The objective of this work is to develop such a model for (m)ethanol-gasoline blends using a simple mixing rule for the ignition delay of alcohol-gasoline blends. The model will be calibrated on pure gasoline (stoichiometric operation) and on pure methanol (stoichiometric operation) and with these two calibrations, the capability of the model to predict knock parameters of methanol-gasoline blends will be investigated.

2. PREDICTIVE KNOCK MODELING

Models to predict the autoignition of unburned mixture in spark-ignition engines range from simple empirical expressions to complex formulations featuring reduced or full chemical kinetics [9]. A widely employed empirical approach is to apply the conservation of delay principle proposed by Livengood and Wu [10]. According to this principle the overall ignition delay time

can be found by integrating its instantaneous value during the compression and combustion stroke. This is analytically expressed by the knock integral reaching unity:

$$\int_{t_{IVC}}^{t_{KO}} \frac{dt}{\tau(t)} = 1 \quad (1)$$

Where t_{IVC} and t_{KO} are the time at intake valve closure and knock onset respectively and $\tau(t)$ is the instantaneous autoignition delay time.

The autoignition delay time τ is the time during which a homogeneous mixture must be maintained at temperature T and pressure p before it autoignites.

The autoignition delay time τ at instantaneous cylinder pressure p, unburned mixture temperature T and composition is typically given by an Arrhenius expression representing the rate limiting step of autoignition:

$$\tau = Ap^n e^{\frac{B}{T}} \quad (2)$$

Where A, n and B are parameters depending on the mixture composition (fuel, Φ, residual gas ratio). The most widely used parameter set for the ignition delay of spark ignition fuels was introduced in 1978 by Douaud and Eyzat based on recording the knock onset in a CFR engine for a range of running conditions and PRFs (primary reference fuels) with octane numbers between 80 and 100 [11].

Another way of calculating the ignition delay is with chemical kinetic models. The drawback for fuel blends is that the kinetic models become very large and complex, with long calculation times as result, and that in many cases no models exist for blends of different fuels.

The Livengood-Wu integral gives an indication of when autoignition will occur in a completely homogeneous mixture. Completely homogeneous mixtures are unlikely in practice and autoignition will be triggered by ‘hot spots’ [12]. Thermal inhomogeneities caused by hot exhaust valves, turbulent transport during compression and large gradients of viscous stresses in

boundary layers can cause these hot spots [12]. This means that autoignition can occur before the Livengood-Wu integral attains a value of unity. As a result, for two-zone thermodynamic engine models, such as the one used in this work, empirical expressions have been shown to yield performance no worse than comprehensive chemical kinetics schemes [9]. The inability of these models to reproduce local hot gas pockets and cyclic variation introduces uncertainties that outweigh those incurred by the simplified chemical kinetics. To consider these effects, multi-zone or 3D CFD approaches are necessary, employing either detailed chemistry or empirical expressions.

Still, the combination of two-zone modeling and the knock integral approach has been confirmed as a useful tool to estimate knock occurrence and intensity, which can be directly linked to the experimentally measured ratio of knocking to non-knocking cycles [13].

2.1. Autoignition correlation for gasoline

The combustion of many hydrocarbon species (gasoline included) exhibits two-stage ignition characteristics. This is especially true for most paraffinic hydrocarbons.

Autoignition correlations are often based on a simple, single-stage Arrhenius expression. These correlations lack detail regarding the cool-flame phenomena.

In the literature, two models were proposed to deal with the two-stage ignition characteristic, discussed below.

2.1.1. The model of Yates et al.

Yates et al. [4], [14] proposed an empirical model concept with a formfitting simplification of the overall ignition delay into four basic steps. These comprised (a) a pre-cool-flame delay at constant temperature, (b) an instantaneous cool-flame temperature increase (which could be

zero), (c) a further delay at constant temperature, and (d) the terminal exothermic auto-ignition. It was assumed that this exothermic reaction sequence could be represented by a simple Arrhenius reaction formulation representing the gross, rate-limiting step, i.e.

$$\tau_h = \phi^{\beta_h} A_h p^{n_h} e^{\frac{\beta_h}{T}} \quad (3)$$

where the temperature profile exhibits a distinct step up at the cool-flame initiation point. The calculation of the overall ignition delay needs to be undertaken in two stages by applying the conservation-of-delay principle proposed by Livengood and Wu, i.e.

$$\int_{t_0}^{t_1} \frac{dt}{\tau_{h,i}} + \int_{t_1}^{t_2} \frac{dt}{\tau_{h,CF}} = 1 \quad (4)$$

where t_1 is defined by the appearance of the cool flame and its associated temperature rise, and t_2 represents the overall ignition delay time. The autoignition delays, $\tau_{h,i}$ and $\tau_{h,CF}$ represent the characteristic exothermic reaction delay evaluated at the initial and post-cool-flame conditions respectively.

If the pressure and temperature are approximated as being constant during each stage, (and taking t_0 as zero), the integral simplifies to:

$$\frac{t_1}{\tau_{h,i}} + \frac{(t_2 - t_1)}{\tau_{h,CF}} = 1 \quad (5)$$

Rearranging, one obtains the overall ignition delay time, t_2, as:

$$t_2 = t_1 + \tau_{h,CF}(1 - \frac{t_1}{\tau_{h,i}}) \quad (6)$$

2.1.2. 3-Arrhenius model proposed by Weisser

This model considers three distinct reaction regimes. The three reaction regimes represent the low, medium and high temperature ignition chemistry. The low and medium temperature reactions occur sequentially, giving rise to a two-stage ignition path. The high temperature reactions lead to a parallel single-stage ignition path [15]. As a result, the overall ignition delay for the full temperature range can be modeled by a simplified system expressed as:

$$\frac{1}{\tau} = \frac{1}{\tau_1+\tau_2} + \frac{1}{\tau_3} \quad (7)$$

where the individual timescales τ_1, τ_2, and τ_3 represent the low, medium and high temperature regime respectively and can be expressed as an Arrhenius-type correlation. This simplified system is illustrated in Figure 1.

2.2. Autoignition correlation for alcohols

Methanol, ethanol, and many aromatic and olefinic molecules do not exhibit a cool flame. Simple single-stage Arrhenius-based models could be employed [4]. For light alcohols and methanol, in particular, a number of correlations were proposed over the years based on shock tube experiments [16, 17], rapid compression machine (RCM) tests [18] and chemical kinetics calculations [4].

A new autoignition correlation for methanol was compared against existing correlations in a previous study of the current authors [13]. In this work, the ignition delay time of methanol-air-residual mixtures was calculated using a chemical kinetics code developed at Eindhoven University of Technology (CHEM1D [19]) and the methanol oxidation mechanism of Li et al. developed at Princeton University [20]. The resulting autoignition delay times were fit as a function of T, p, Φ and residual gas content f using a correlation form similar to that of Douaud and Eyzat [11] (see Eq. 2) with the effects of Φ and f implemented similarly to previous work [3, 21]; in the pre-exponential factor A:

$$A = A_0 \varphi^{\beta} (1 + f)^{m} \quad (8)$$

Where A_0 and β are constants. Based on analysis of the calculated data, the pressure exponent n, dilution exponent m and activation temperature B were fit as a polynomial function of Φ, T and f.

This newly developed autoignition delay correlation was able to capture the high temperature sensitivity of methanol autoignition kinetics. This resulted in a better prediction of the knock limited spark advance for variations in compression ratio and load [13]. As a result, this autoignition correlation for methanol will be used in this study.

2.3. Autoignition correlation for alcohol-blends

A possible solution to calculate the ignition delay of binary or more complex alcohol-gasoline blends would be to have mixing rules which can determine the ignition delay of fuel blends out of the ignition delay of the fuel components.

To find a mixing rule, an accurate determination of the ignition delay of the fuel components and the ignition delay of the fuel blends is needed. There are few experimental measurements of alcohol fuel blends [22-24] and there can be doubt on the accuracy of the measurements when measurements are compared, see Figure 2 where the ignition delays of ethanol [25] and an ethanol/iso-octane blends [22] are plotted for the same conditions.

In this study, we used the empirical model of Yates et al. [4] to calculate the ignition delays of blends of primary reference fuels and methanol to investigate if a simple mixing rule could be applied to calculate the ignition delays of alcohol-hydrocarbon blends. Over 1500 detailed chemical kinetic simulations were used to calibrate the model of Yates el al. [4], enabling it to encompass a full range of PRF blends and methanol blends. The standard deviation of the overall ignition delay prediction was about 11%.

The simplest mixing rules are based on mole, mass, volume or energy fraction:

$$\tau_{blend} = \sum_{i=1}^{n} \alpha_i . \tau_i \quad (9)$$

In the previous expression α_i is either the mole fraction, mass fraction, volume fraction or energy fraction of the fuel components. The energy fraction can be calculated as follows:

$$\alpha_i = \frac{\Delta cH_i^{\circ}.x_i}{\sum_{i=1}^{n} \Delta cH_i^{\circ}.x_i} \quad (10)$$

$cH_i°$ is the heat of combustion of the mixture components. x_i is the mole fraction of the fuel components.

In Figure 3, the mixing rule based on volume fraction was used to predict the ignition delay of a blend of methanol and a PRF fuel. As can be seen, this rule overpredicts the ignition delay for lower temperatures because of the very different values for the ignition delay of methanol and the PRF fuel due to the cool flame behavior of the PRF fuel.

This could be solved by using logarithmic values of the ignition delay as follows:

$$\tau_{blend} = \sum_{i=1}^{n} \alpha_i . \log(\tau_i) \quad (11)$$

or

$$\tau_{blend} = \prod_{i=1}^{n} \tau_i^{\alpha_i} \quad (12)$$

In Figure 4, this mixing rule is used with the mole and energy fractions of the different fuels. Similar to the mixing rules for laminar burning velocity of methanol-gasoline blends, the energy fraction mixing rule has the best agreement [26, 27].

As a result, this study will test the validity of the mixing rule based on the energy fraction with the logarithmic values of the ignition delay. For the ignition delay of pure methanol, the correlation of Vancoillie et al. [13] will be used and for the ignition delay of gasoline, the model of Yates et al. [4] will be used.

3. EXPERIMENTAL WORK

3.1. Engine

To analyze the combustion model's predictive capabilities for knock, a series of measurements were done on a port fuel injected single cylinder CFR engine, described in [28]. The main characteristics of this engine are summarized in Table 1.

The measurements of knock comprise various lambda values and methanol-gasoline ratios. Measurements were done for M0, M50 and M75 at lambda equal to 1, 1.2 and 0.8 and for pure methanol at lambda equal to 1 and 1.2. The compression ratio was fixed at 9, ignition timing sweeps were performed from non-knocking operation to 100% knock with the throttle opening fixed at 27.5° resulting in an IMEP range from 7.2 to 9 bar and volumetric efficiencies between 83% and 85%. In order to allow an accurate comparison, all measurements were performed on the same day and all parameters were fixed except for the injection duration, ignition timing and the fuel composition.

3.2. Knock detection

To validate the proposed knock prediction model, it is crucial to have a knock detection method that can accurately separate knocking from non-knocking cycles and detects the onset of knock oscillations and their intensity for knocking cycles.

There are plenty of well established methods to detect knock from the cylinder pressure trace. Some are based on the raw pressure trace, employing maximum values of the first, second or third derivatives of this signal, or the heat release rate derived from it, as measures of knock intensity. Other methods use the (band/high pass) filtered pressure trace or heat release rate to calculate knock intensities based on the maximum amplitude or signal energy of the pressure or heat release rate oscillations [29].

A number of algorithms were tested in a previous study [13] and the knock detection method of Worret et al. [30] was selected because it correctly captures knock onset, regardless of variations

in Φ, compression ratio, throttle position and ignition timing and could also discern light knocking cycles.

The cycle-resolved knock detection algorithm of Worret et al. [30] is based on the band-pass filtered heat release rate (3-17 kHz pass band in this work) and builds on popular MAPO (Maximum Amplitude of Pressure Oscillations) and SEPO (Signal Energy of Pressure Oscillations) methods.

Knock intensities, calculated based on the integrated signal energy of the filtered heat release rate, are determined before and after a potential knock onset to differentiate between knocking oscillations and non-knocking signal noise (see Figure 5). Starting from the location of the maximum amplitude of the heat release rate oscillations, knock onset is detected as the first crank angle position where a certain threshold value is exceeded in the filtered heat release rate (see Figure 5). The algorithm was implemented as described in [30] and no further adjustment to threshold values or other constants proved necessary throughout the measurement range.

The relevant quantities resulting from the knock analysis are the ratio of knocking cycles to the total number of logged cycles, the average values and standard deviation of knock intensity and crank angle of knock onset for the knocking cycles.

As an example Figure 6 shows these values plotted as a function of spark advance for stoichiometric fuel-air mixtures of pure gasoline, M50 and pure methanol. It can be seen that as the methanol ratio in the fuel rises from zero to 100% (while the lambda value and throttle position remain constant) the knock ratio exceeds the 10% threshold at more advanced spark timing. Knock intensities also rise as a function of spark advance and knock onset occurs earlier in the cycle for higher methanol fraction because of the more advanced spark timing.

For reference, the standard deviations of knock intensity and knock onset position have been added to the plots. As can be seen, the knock intensity is particularly cycle dependent. Increasing

the number of logged cycles might help to reduce its standard deviation. The uncertainty in knock onset time is in the range of 1.5-2.5 °ca for most the cases, which is about the order of magnitude of variations due to knock onset position, pressure transducer position and the speed of sound [31].

4. SIMULATION RESULTS

4.1. Model setup

The knock integral framework employing the autoignition delay time correlations of Yates et al. and Vancoillie et al. was implemented in a commercial engine simulation code (GT-Power [32]) in order to assess its predictive performance.

To simulate the conditions as measured on the CFR engine, an engine model was built focusing on the cylinder:

- The measured intake and exhaust runner temperature and pressure traces were used as boundary conditions. This reduces the uncertainty on in-cylinder mixture conditions compared to calculating this information from a gas dynamics model of the complete intake and exhaust geometry.
- The intake mixture was completely evaporated methanol/gasoline-air with the measured lambda value.
- The residual gas content followed from the simulation.
- The heat transfer was calculated using the model of Woschni and the unburned mixture was treated as a single zone.
- The temperatures of burned and unburned mixture were calculated based on conservation of mass and energy, as explained in [33].

- In order to obtain the same in-cylinder pressure as measured on the engine, the applied burn rates were those resulting from a heat release rate analysis of the measured pressure trace that best corresponded to the average cylinder pressure trace (average of 100 cycles).

The Woschni calibration constant for compression and expansion were chosen for best correspondence between measured and simulated cylinder pressure traces during compression and expansion. The Woschni coefficient during combustion was chosen by ensuring the energy balance between the injected fuel energy and released heat. As a result, the effects of evaporating fuel, the effects of blowby, crevice mass and incomplete combustion will be lumped into this parameter. All Woschni coefficients were kept the same for all simulated cases.

The knock prediction model was calibrated by multiplying the knock ignition delay correlation with a factor in order to get autoignition onset exactly at the measured crank angle for a certain reference condition. In this study, this was done for stoichiometric operation at knock limited spark advance for both gasoline and methanol. The calibration factor for the ignition delay correlation of gasoline (Yates et al.) was 0.714 and the calibration factor for the ignition delay correlation of methanol (Vancoillie et al.) was 0.128.

The multipliers for the new correlation and that of Yates et al. are markedly low, indicating that the calculated ignition delay is too high. This could be expected since these correlations do not have the effect of hot spots lumped into the correlation's constants which is the case for the correlation of Douaud & Eyzat which was calibrated by engine experiments [13]. Another way of calibrating these correlations would be to artificially increase the unburned mixture temperature to represent hot spots in the unburned mixture [34].

4.2. Knock limited spark advance

A crucial performance indicator of the knock prediction models is their ability to distinguish between knocking and non-knocking conditions and predict the knock limited spark advance (KLSA). In this work, the experimental KLSA is taken to be the least advanced spark timing at which the knock ratio is more than 10%. The simulated KLSA is the least advanced spark timing at which the knock integral exceeds 1 before the end of combustion. As the spark timing was experimentally varied in steps of 1 or 2 °ca, the uncertainty on the KLSA is at least 1 or 2 °ca.

In Figure 7, the experimental and simulated values for KLSA are plotted as a function of the blend ratio. It can be seen that for stoichiometric, lean and rich mixtures, the experimental KLSA is more advanced than the simulated KLSA. The knock integral exceeds 1 before the end of combustion at less advanced spark timing than the experimental KLSA. This can also be seen in Figure 9 where the difference between the measured and simulated KLSA is plotted as a function of the blend ratio. To detect knock, the oscillations resulting from the autoignition of the unburned air-fuel mixture have to be detectable. As mentioned by Richard et al. [35], the influence of the cylinder volume at the instant of knock occurrence could be important. The oscillations are less intense the further knock occurs from top dead center. Secondly, the amount of unburned mixture at the time of autoignition might have an influence on the knock intensity [13]. As a result, it could happen that the conditions for autoignition are met but there is no detection of knock because the knock onset is too far from the top dead center or the unburned mixture mass at knock onset is too small. Therefore, a second condition was used in this study to identify knock: there is no knock if the knock onset is too far from the top dead center unless the amount of unburned mixture is large and there is no knock if the amount of unburned mixture at

knock onset is too small unless it is very close to the top dead center. The following condition was used.

There is knock if :

- The knock integral exceeds 1 before the end of combustion
- Additional condition: $\left|\frac{25}{\theta_{KO}}.\frac{m_{frac,u}}{0.1}\right| > 1$

Where $m_{frac,u}$ is the simulated unburned mass fraction and θ_{KO} is the simulated crank angle at knock onset. In this study, the unburned mass fraction was used and not the total amount of unburned mixture because the differences in volumetric efficiencies are very small. For load variations with significantly different volumetric efficiencies, the total amount of unburned mixture instead of the unburned mixture fraction might be important. With the measurement done for this study, the influence of engine speed could not be investigated, as well as the influence of the compression ratio. Both properties will have an influence and should probably be included in the additional condition for knock detection.

In Figure 8 and Figure 9, the results can be seen with the additional condition. The simulated KLSA is now closer to the experimental KLSA, especially for the stoichiometric and lean mixtures.

4.3. Knock integral at the experimental Knock Onset

Another indication of the model's performance is the value of the knock integral at the experimental knock onset. In Figure 10, the value of knock integral can be seen at the experimental knock onset for gasoline, M50 and pure methanol. Only the measurements for which the knock ratio is more than 10% are shown. It can be seen that with more advanced spark timing the knock integral at knock onset increases for most cases. This increase is stronger for

pure methanol than for pure gasoline. This is probably due to the fact that the ignition timing is very different for the measurements on methanol compared to gasoline while the Woschni coefficients of the heat transfer model were kept the same for all simulated cases. The increase of the value of the knock integral with more advanced spark timing is also probably due to an underestimated heat transfer by the Woschni model during knock [36]. Heat flux measurements could help to investigate this problem.

Heat flux measurements will be part of future research in order to investigate both the evaporative cooling effect and the wall heat transfer. The same measurement techniques can be used as in [28].

4.4. Knock intensity

The problem of knock is that it induces damage. The higher the knock intensity, the higher the probability of knock induced damage. As a result, the knock intensity is an important parameter for the design and calibration of the engine. A possible equation for knock intensity was proposed by Bougrine et al. [3].

$$KI = K_1 \left(1 - \frac{m_{frac,b}}{\max(1,\phi)}\right)(CR - 1)\sqrt{1 - \frac{\theta_{KO}}{K_2}}.rpm \quad (13)$$

Where K_1 is a calibration constant, K_2 is the maximum crank angle at which knock is still audible (set to 40 °ca ATDC), $m_{frac,b}$ is the burned mass fraction and θ_{KO} is the crank angle of knock onset. In Figure 11, the part of the knock intensity equation that changes for the measurements performed during this study, $\left(1 - \frac{m_{frac,b}}{\max(1,\phi)}\right)\sqrt{1 - \frac{\theta_{KO}}{K_2}}$, and the knock intensity that was derived from the knock detection algorithm of Worret et al. [30] are plotted as a function of the spark timing. A calibration constant was used to rescale this part of the equation in order to have the same knock intensity as gasoline at KLSA as was derived from the knock

detection algorithm. The same calibration constant was then also used for the gasoline-methanol blends as well as for pure methanol.

It can be seen that the equation proposed by Bougrine et al. underpredicts the knock intensity when it is compared to the knock intensity from the knock detection algorithm of Worret el al. [30].

This equation does not take into account the pressure and temperature at knock onset. This could be important because the temperature and the pressure will change going from gasoline to methanol and both the temperature and pressure have an influence on the gas properties and as a result on the knock oscillations. This could be taken into account by entering the crank angle of knock onset at KLSA into the equation as this reflects the necessary conditions for autoignition of the fuel which are influenced by temperature and pressure. Instead of using $\sqrt{1-\frac{\theta_{KO}}{K_2}}$, this could be done as follows:

$$\left(1-\frac{m_{frac,b}}{\max(1,\phi)}\right).\left(\frac{\theta_{KO,KLSA}+2-\theta_{knock}}{\theta_{KO}-\theta_{knock}}-1\right) \quad (14)$$

Where $\theta_{KO,KLSA}$ is the crank angle of knock onset at KLSA, θ_{KO} is the crank angle of knock onset for the current spark timing and θ_{knock} is the crank angle of knock onset which would be the worst for the intensity of the knock if knock onset was to occur at that crank angle (set to -10 °ca ATDC). The number '2' is entered into the equation to make sure that the knock intensity is not equal to zero at KLSA and this can be interpreted as the knock intensity being zero when the spark advance is retarded with 2° ca at KLSA.

The results are plotted on the same figures (Figure 10) as for the Knock Intensity calculated with the equation of Bougrine et al. The values of the newly developed knock intensity equation (marked with Sileghem) were also rescaled in order to have the same knock intensity as gasoline

at KLSA as was derived from the knock detection algorithm. As can be seen on the Figure 10, there is a better agreement with the experimental trends. This should however be further investigated for load and engine speed sweeps.

4.5. Knock onset crank angle

A last test of the knock prediction models is their ability to reproduce the correct crank angle of knock onset (θ_{KO}). Although this quantity is not of direct use to engine designers, it has an effect on the knock intensity. Figures 12, 13 and 14 show the experimental and simulated crank angle of knock onset for a spark timing sweep. In Figure 12, the results are shown for stoichiometric operation, in Figure 13 for lean operation and in Figure 14 for rich operation. Almost all the knock onsets are predicted within the error margins of the experimental knock onset. A consistent trend for all cases is that the simulated knock onset advances faster with spark advance than the experimental knock onset. This could again be due to an underestimated heat transfer by the Woschni model during knock and heat flux measurements could help to investigate this issue.

Figure 15 shows a comparison made between simulated results for stoichiometric, lean and rich operation on M50 where the energy fraction mixing rule together with the logarithmic value of the ignition delays is used as well as a mixing rule based on the volumetric fractions and real values of the ignition delay. This mixing rule generally underpredicts knock more than the energy fraction mixing rule with logarithmic values which could be expected looking at the ignition delay calculated with the volume fraction mixing rules in Figure 3. As a result, for the lean mixtures, the simulated KLSA was 2 degrees earlier than the experimental KLSA. The

simulated results for knock onset are still reasonable but the differences are larger and outside of the error bars, closer to less advanced spark timing (closer to KLSA).

5. CONCLUSIONS

In order to better understand and predict the knock behavior of alcohol blends, a mixing rule for the autoignition delay time of alcohol-gasoline blends was proposed. This energy-based mixing rule was used together with an autoignition delay time correlation of gasoline and an autoignition delay time correlation of methanol in a knock integral model that was implemented in a two-zone engine code.

To validate the proposed model, knock occurrence was experimentally investigated on a CFR engine for four methanol-gasoline blends (gasoline, M50, M75 and M100).

Experimental metrics of knock included knock limited spark advance (KLSA), fraction of knocking cycles, knock onset timing and knock intensity based on signal energy of heat release rate oscillations.

The proposed correlation and knock integral approach performed satisfactorily despite the gross simplification associated with two-zone modeling (no hot spots, no cyclic variation). The experimental KLSA was more advanced than the simulated KLSA. The knock integral exceeded 1 before the end of combustion at less advanced spark timing than the experimental KLSA. Therefore, a second condition was used in this study to identify knock based on unburned mass fraction and the crank angle at knock onset which gave better agreement. Secondly, the agreement between the simulated knock intensity and the experimental knock intensity was better if the crank angle of knock onset at KLSA was taken into account as this reflects the necessary conditions for autoignition of the fuel which are influenced by temperature and

pressure. Finally, the model was able to predict almost all the knock onsets within the error margins of the experimental knock onset.

Further model improvement should focus on better capturing the effects of evaporation cooling and wall heat transfer with heat flux measurements. This will be the subject of future work, together with validation of the current model at different operating conditions.

ACKNOWLEDGEMENTS - L. Sileghem gratefully acknowledges a Ph. D. fellowship of the Research Foundation - Flanders (FWO11/ASP/056). The authors would like to thank BioMCN for providing the bio-methanol used in this study.

REFERENCES

[1] B. Iosefa, Methanol fuels: igniting global growth, in: 20th International Symposium on Alcohol Fuels (ISAF), Stellenbosch, South Africa, 2013.
[2] J.B. Heywood, Internal Combustion Engine Fundamentals, MacGraw-Hill, New York, 1988.
[3] Bougrine, S., Richard, S., and Veynante, D., "Modelling and Simulation of the Combustion of Ethanol blended Fuels in a SI Engine using a 0D Coherent Flame Model," SAE Technical Paper 2009-24-0016, 2009, doi:10.4271/2009-24-0016.
[4] A. Yates, A. Bell, A. Swarts, Insights relating to the autoignition characteristics of alcohol fuels, Fuel, 89 (2010) 83-93.
[5] J. Warnatz, U. Maas, R.W. Dibble, Combustion: Physical and Chemical Fundamentals, Modeling and Simulation, Experiments, Pollutant Formation, Springer-Verlag, Berlin, Germany, 1996.
[6] Stein, R., Polovina, D., Roth, K., Foster, M. et al., "Effect of Heat of Vaporization, Chemical Octane, and Sensitivity on Knock Limit for Ethanol - Gasoline Blends," *SAE Int. J. Fuels Lubr.* 5(2):823-843, 2012, doi:10.4271/2012-01-1277.
[7] Vancoillie, J., Verhelst, S., and Demuynck, J., "Laminar Burning Velocity Correlations for Methanol-Air and Ethanol-Air Mixtures Valid at SI Engine Conditions," SAE Technical Paper 2011-01-0846, 2011, doi:10.4271/2011-01-0846.
[8] Nakata, K., Utsumi, S., Ota, A., Kawatake, K. et al., "The Effect of Ethanol Fuel on a Spark Ignition Engine," SAE Technical Paper 2006-01-3380, 2006, doi:10.4271/2006-01-3380.
[9] Burluka, A., Liu, K., Sheppard, C., Smallbone, A. et al., "The Influence of Simulated Residual and NO Concentrations on Knock Onset for PRFs and Gasolines," SAE Technical Paper 2004-01-2998, 2004, doi:10.4271/2004-01-2998.
[10] J.C. Livengood, P.C. Wu, Correlation of autoignition phenomena in internal combustion engines and rapid compression machines, Symposium (International) on Combustion, 5 (1955) 347-356.
[11] Douaud, A. and Eyzat, P., "Four-Octane-Number Method for Predicting the Anti-Knock Behavior of Fuels and Engines," SAE Technical Paper 780080, 1978, doi:10.4271/780080.

[12] D. Bradley, G.T. Kalghatgi, Influence of autoignition delay time characteristics of different fuels on pressure waves and knock in reciprocating engines, Combustion and Flame, 156 (2009) 2307-2318.
[13] Vancoillie, J., Sileghem, L., and Verhelst, S., "Development and Validation of a Knock Prediction Model for Methanol-Fuelled SI Engines," SAE Technical Paper 2013-01-1312, 2013, doi:10.4271/2013-01-1312.
[14] Yates, A. and Viljoen, C., "An Improved Empirical Model for Describing Auto-ignition," SAE Technical Paper 2008-01-1629, 2008, doi:10.4271/2008-01-1629.
[15] A. Vandersickel, M. Hartmann, K. Vogel, Y.M. Wright, M. Fikri, R. Starke, C. Schulz, K. Boulouchos, The autoignition of practical fuels at HCCI conditions: High-pressure shock tube experiments and phenomenological modeling, Fuel, 93 (2012) 492-501.
[16] C.T. Bowman, Shock-Tube Investigation Of High-Temperature Oxidation Of Methanol, Combustion and Flame, 25 (1975) 343-354.
[17] K. Natarajan, K.A. Bhaskaran, An experimental and analytical study of methanol ignition behind shock waves, Combust. Flame, 43 (1981) 35-49.
[18] K. Kumar, C.-J. Sung, Autoignition of methanol: Experiments and computations, Int. J. Chem. Kinet., 43 (2011) 175-184.
[19] Combustion Technology group, Eindhoven University of Technology. CHEM1D. 1994 [cited 2010 May 20th]; Available from: http://w3.wtb.tue.nl/en/research/research_groups/combustion_technology/research/flamecodes/chem1d/.
[20] J. Li, Z.W. Zhao, A. Kazakov, M. Chaos, F.L. Dryer, J.J. Scire, A comprehensive kinetic mechanism for CO, CH2O, and CH3OH combustion, Int. J. Chem. Kinet., 39 (2007) 109-136.
[21] Syed, I., Mukherjee, A., and Naber, J., "Numerical Simulation of Autoignition of Gasoline-Ethanol/Air Mixtures under Different Conditions of Pressure, Temperature, Dilution, and Equivalence Ratio.," SAE Technical Paper 2011-01-0341, 2011, doi:10.4271/2011-01-0341.
[22] L.R. Cancino, M. Fikri, A.A.M. Oliveira, C. Schulz, Ignition delay times of ethanol-containing multi-component gasoline surrogates: Shock-tube experiments and detailed modeling, Fuel, 90 (2011) 1238-1244.
[23] L.R. Cancino, M. Fikri, A.A.M. Oliveira, C. Schulz, Autoignition of gasoline surrogate mixtures at intermediate temperatures and high pressures: Experimental and numerical approaches, Proceedings of the Combustion Institute, 32 (2009) 501-508.
[24] Z. Jiaxiang, N. Shaodong, Z. Yingjia, T. Chenglong, J. Xue, H. Erjiang, H. Zuohua, Experimental and modeling study of the auto-ignition of n-heptane/n-butanol mixtures, Combustion and Flame, 160 (2013) 31-39.
[25] L.R. Cancino, M. Fikri, A.A.M. Oliveira, C. Schulz, Measurement and Chemical Kinetics Modeling of Shock-Induced Ignition of Ethanol-Air Mixtures, Energy & Fuels, 24 (2010) 2830-2840.
[26] L. Sileghem, J. Vancoillie, J. Demuynck, J. Galle, S. Verhelst, Alternative Fuels for Spark-Ignition Engines: Mixing Rules for the Laminar Burning Velocity of Gasoline–Alcohol Blends, Energy & Fuels, 26 (2012) 4721-4727.
[27] L. Sileghem, V.A. Alekseev, J. Vancoillie, E.J.K. Nilsson, S. Verhelst, A.A. Konnov, Laminar burning velocities of primary reference fuels and simple alcohols, Fuel, 115 (2014) 32-40.
[28] J. Demuynck, M. De Paepe, H. Huisseune, R. Sierens, J. Vancoillie, S. Verhelst, Investigation of the influence of engine settings on the heat flux in a hydrogen- and methane-fueled spark ignition engine, Applied Thermal Engineering, 31 (2011) 1220-1228.
[29] Lämmle, C., "Numerical and Experimental Study of Flame Propagation and Knock in a Compressed Natural Gas Engine", Doctor of Technical Sciences, 2005.

[30] Worret, R., Bernhardt, S., Schwarz, F., and Spicher, U., "Application of Different Cylinder Pressure Based Knock Detection Methods in Spark Ignition Engines," SAE Technical Paper 2002-01-1668, 2002, doi:10.4271/2002-01-1668.
[31] C. Elmqvist, F. Lindström, H.-E. Ångström, B. Grandin, G. Kalghatgi, Optimizing Engine Concepts by Using a Simple Model for Knock Prediction in, 2003.
[32] GammaTechnologies, GT-Suite Version 7.0 User's Manual in, Westmont, IL, USA, 2009.
[33] S. Verhelst, C.G.W. Sheppard, Multi-zone thermodynamic modelling of spark-ignition engine combustion - An overview, Energy Conversion and Management, 50 (2009) 1326-1335.
[34] Bromberg, L. and P. Blumberg, "Estimates of DI Hydrous Ethanol Utilization for Knock Avoidance and Comparison to a Measured and Simulated DI E85 Baseline", MIT Plasma Science and Fusion Center, Cambridge, MA, 2009.
[35] S. Richard, S. Bougrine, G. Font, F.-A. Lafossas, F.L. Berr, On the Reduction of a 3D CFD Combustion Model to Build a Physical 0D Model for Simulating Heat Release, Knock and Pollutants in SI Engines, Oil and Gas Science and Technology - Rev. IFP, 64 (2009) 223-242.
[36] Demuynck, J., Chana, K., De Paepe, M., and Verhelst, S., "Evaluation of a Flow-Field-Based Heat Transfer Model for Premixed Spark-Ignition Engines on Hydrogen," SAE Technical Paper 2013-01-0225, 2013, doi:10.4271/2013-01-0225.

Figure 7: Measured and simulated knock limited spark advance (KLSA) as a function of the blend ratio. Simulation based only on the knock integral.

Figure 8: Measured and simulated knock limited spark advance (KLSA) as a function of the blend ratio. Simulation based on the knock integral + additional condition.

Figure 9: Differences between the measured and simulated knock limited spark advance (KLSA) as a function of the blend ratio. ———: Simulation based on the knock integral; - - - - -: Simulation based on the knock integral + additional condition.

Figure 10: Knock integral at the experimental knock onset for gasoline, M50 and methanol as a function of the ignition timing.

Figure 11: Measured and simulated knock intensity for stoichiometric mixtures.

Figure 12: Knock Onset stoichiometric mixtures

Figure 13: Knock Onset lean mixtures

Figure 14: Knock Onset rich mixtures

Figure 15: Knock Onset: Comparison between the energy fraction mixing rule with logarithmic value and volume fraction mixing rule with real values.

Bore	82.55 mm
Stroke	114.2 mm
Swept Volume	611.7 cm^3
Geometry	Disc-shaped
Speed	600 rpm
IVO/IVC	17 °CA ATDC / 26 °CA ABDC
EVO/EVC	32 °CA BBDC / 6°CA ATDC

Table 1: Characteristics of the single cylinder CFR engine

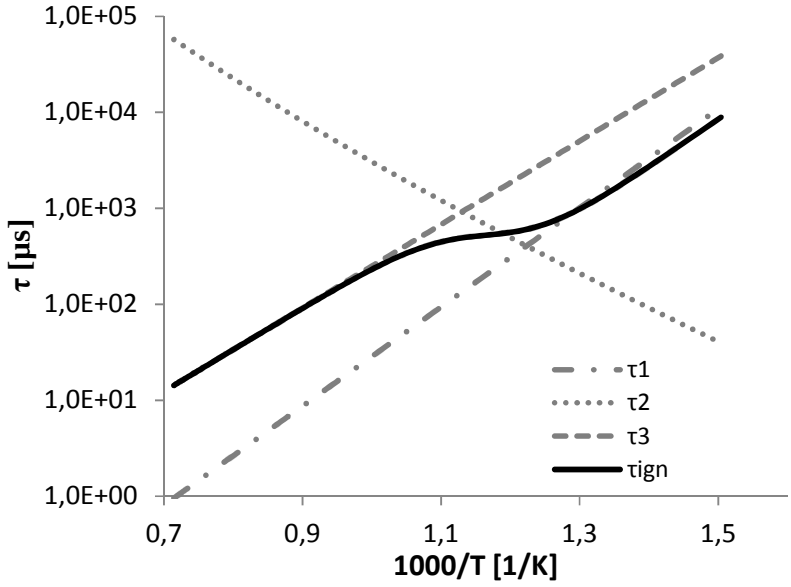

Figure 1 – Illustration of the 3-Arrhenius model proposed by Weisser

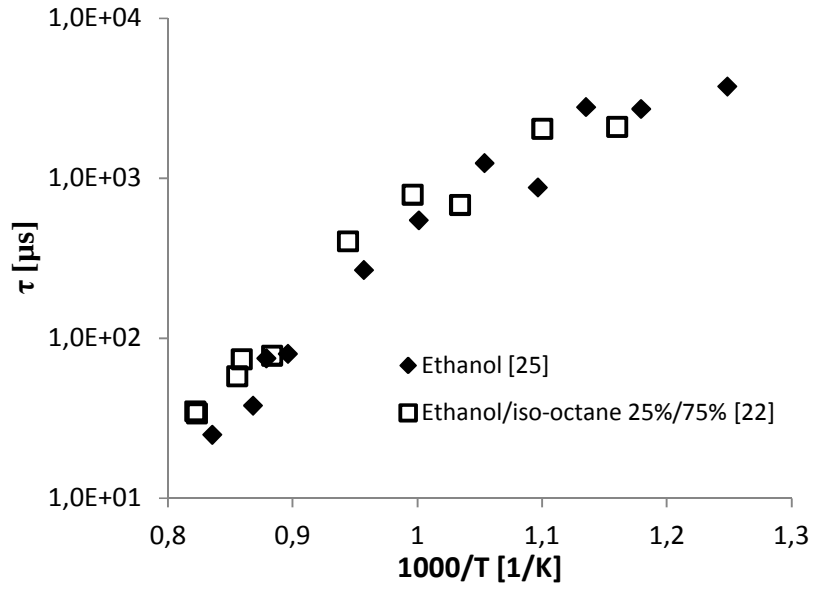

Figure 2 - Ignition delay times of stoichiometric ethanol-air mixtures and ethanol/iso-octane mixtures at 30 bar [22, 25]

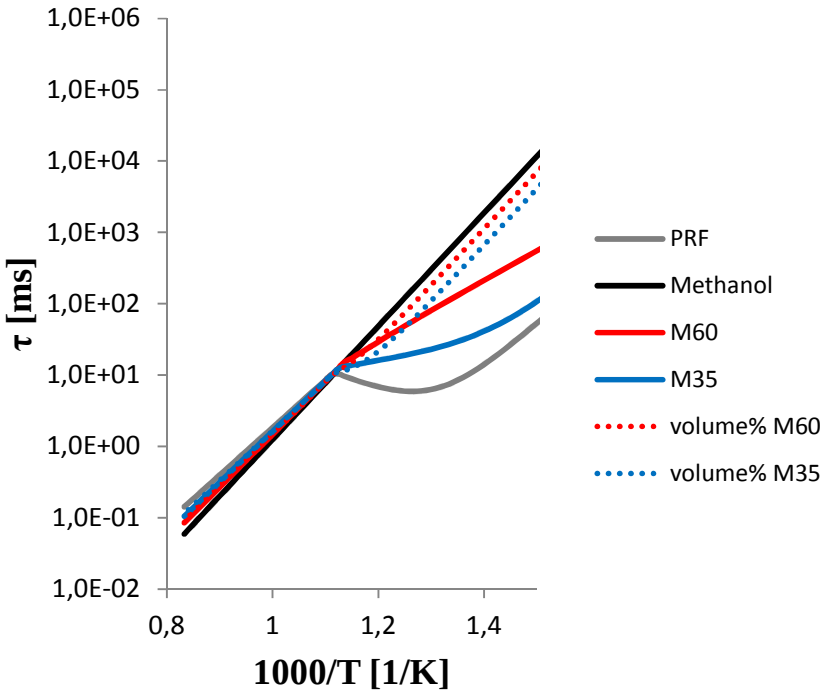

Figure 3 – Ignition delays of methanol, PRF80 and methanol/PRF blends calculated with the model of Yates et al. [4, 14] and ignition delays calculated with the volume fraction mixing rule

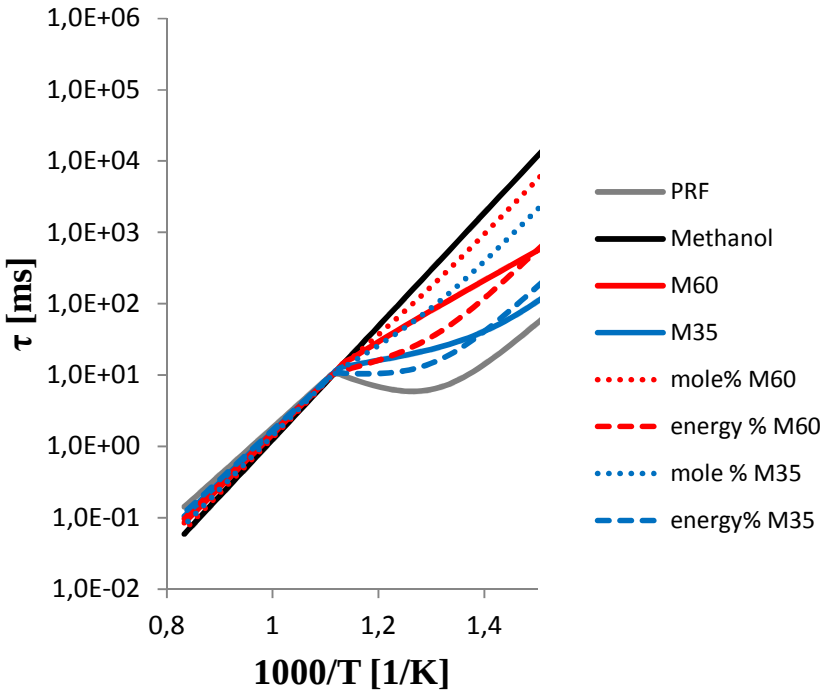

Figure 4 -Ignition delays of methanol, PRF80 and methanol/PRF blends calculated with the model of Yates et al. [4, 14] and ignition delays calculated with the mole and energy fraction mixing rule (logarithmic values)

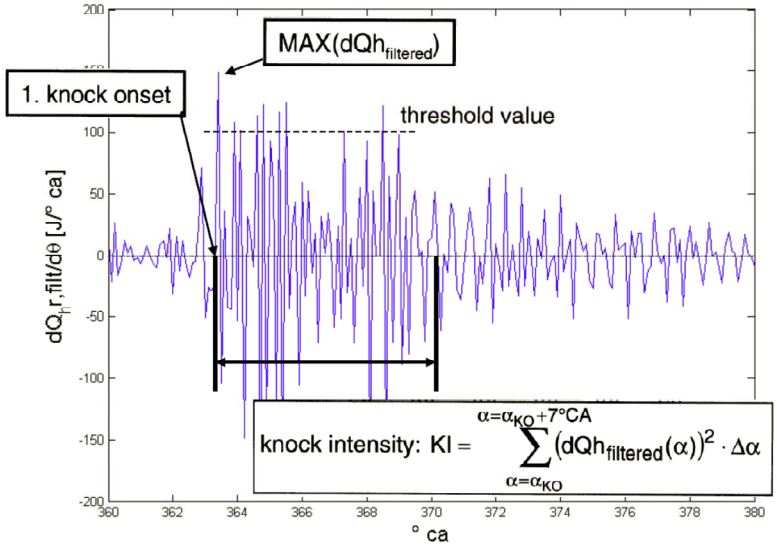

Figure 5: Application example of the knock detection algorithm of Worret et al. [30]

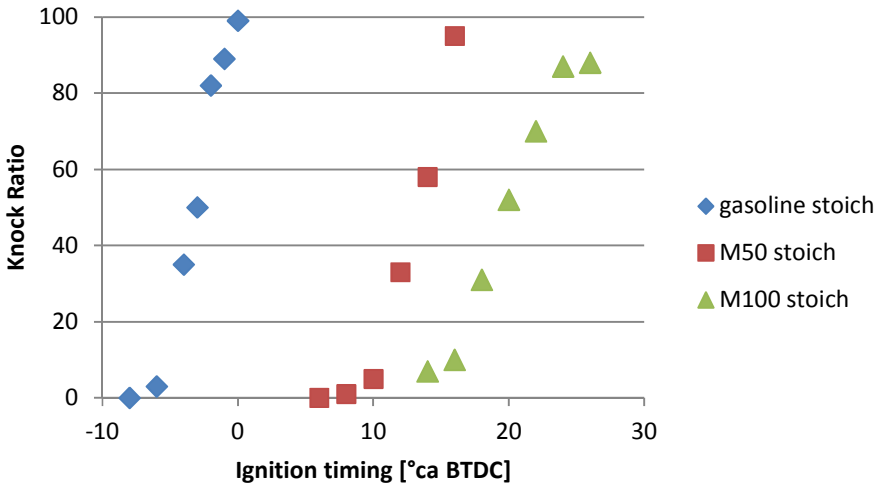
Knock Ratio
100
80
60
40
20
0
-10
0
10
20
30
Ignition timing [°ca BTDC]
gasoline stoich
M50 stoich
M100 stoich

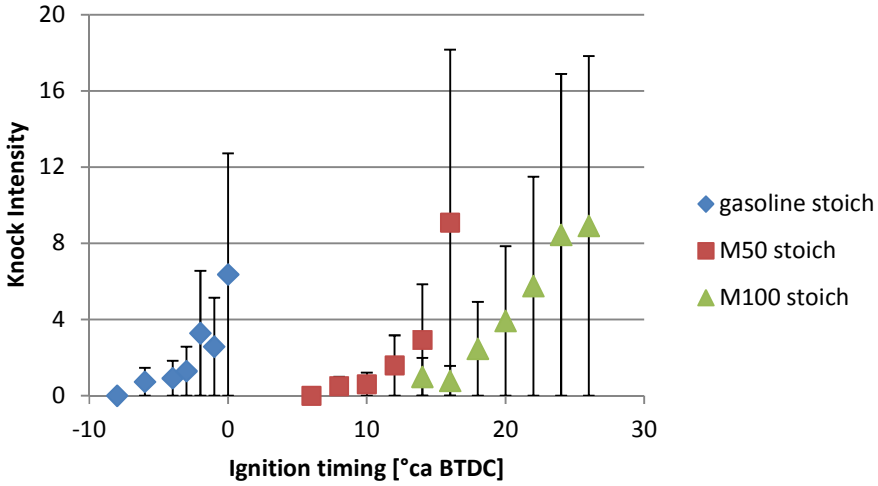
Knock Intensity
20
16
12
8
4
0
-10
0
10
20
30
Ignition timing [°ca BTDC]
gasoline stoich
M50 stoich
M100 stoich

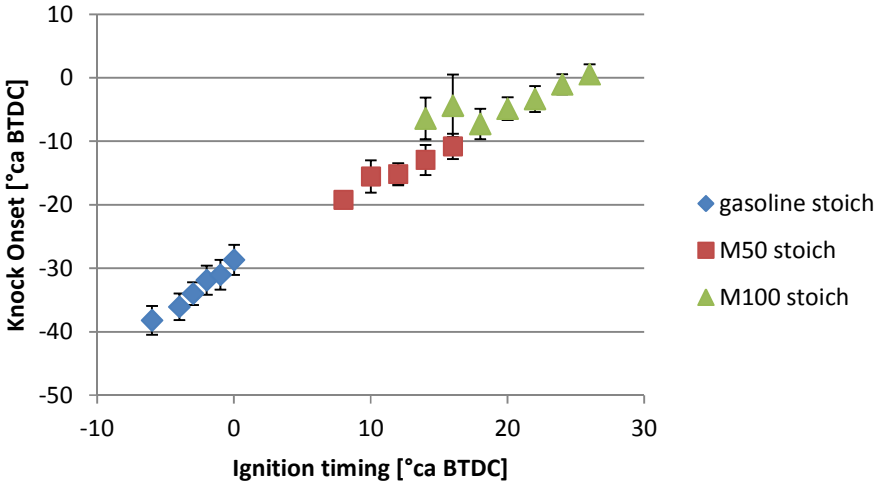
Knock Onset [°ca BTDC]
10
0
-10
-20
-30
-40
-50
-10
0
10
20
30
Ignition timing [°ca BTDC]
gasoline stoich
M50 stoich
M100 stoich

Figure 6 – Measured knock ratios, knock intensities and knock onsets for stoichiometric operation on gasoline, M50 and methanol

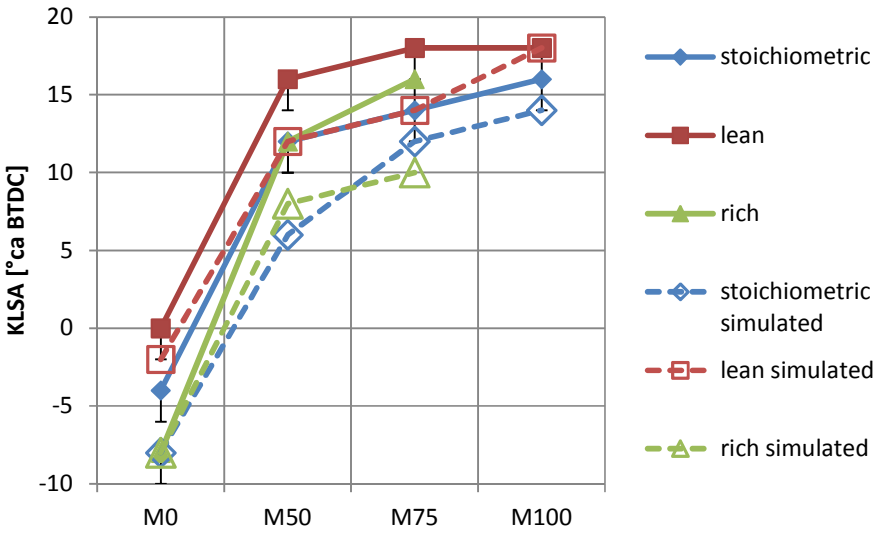

Figure 7 - Measured and simulated knock limited spark advance (KLSA) as a function of the blend ratio. Simulation based only on the knock integral.

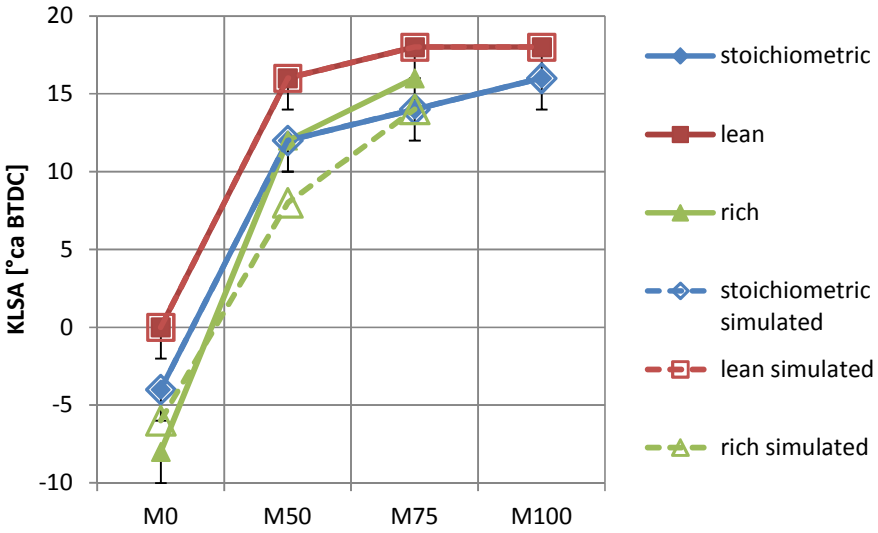

Figure 8 - Measured and simulated knock limited spark advance (KLSA) as a function of the blend ratio. Simulation based on the knock integral + additional condition.

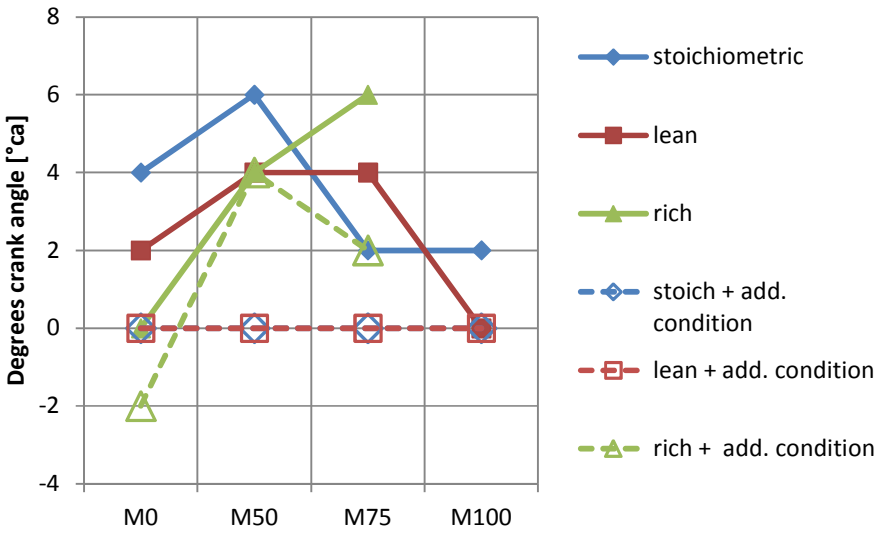

Figure 9 – Differences between the measured and simulated knock limited spark advance (KLSA) as a function of the blend ratio. ———: Simulation based on the knock integral; - - - -: Simulation based on the knock integral + additional condition.

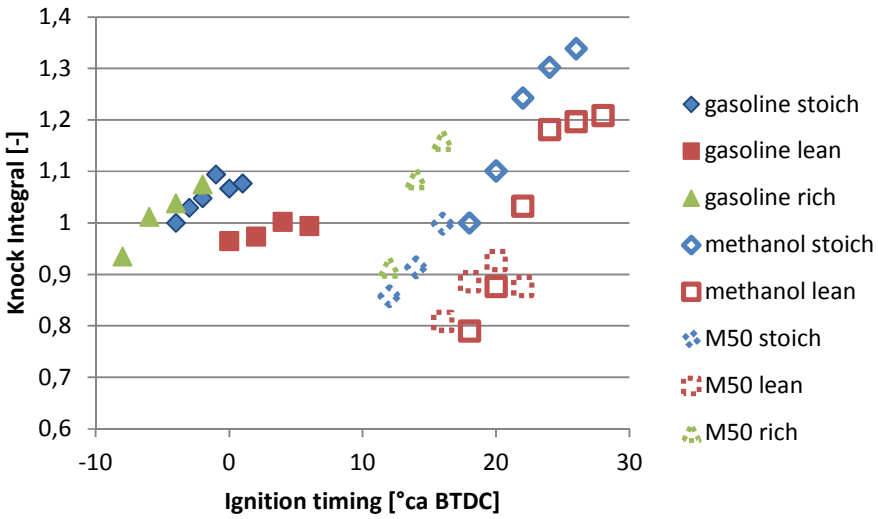

Figure 10 – Knock integral at the experimental knock onset for gasoline, M50 and methanol as a function of the ignition timing.

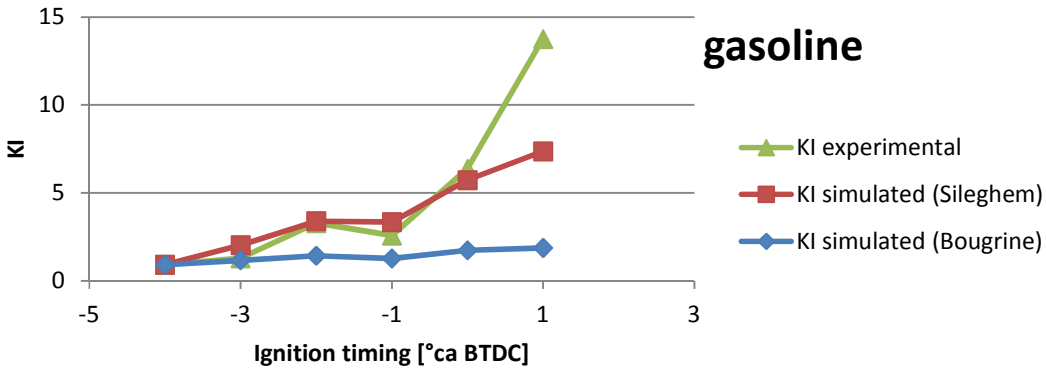
gasoline
KI
15
10
5
0
-5
-3
-1
1
3
Ignition timing [°ca BTDC]
KI experimental
KI simulated (Sileghem)
KI simulated (Bougrine)

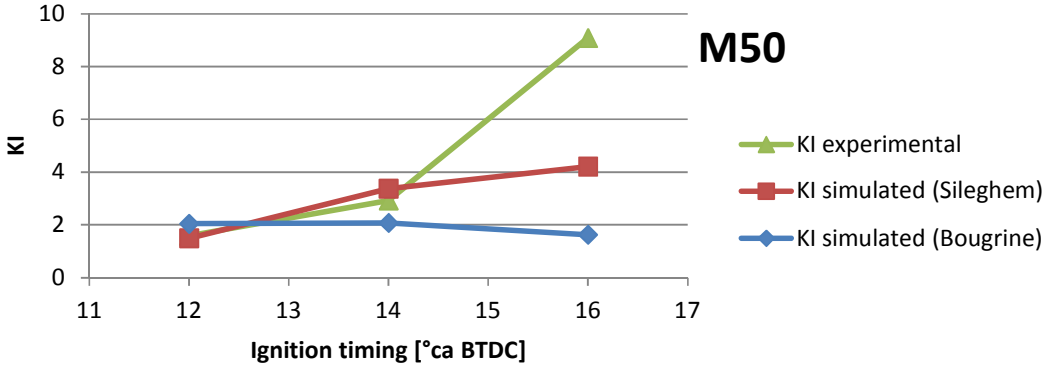
M50
KI
10
8
6
4
2
0
11
12
13
14
15
16
17
Ignition timing [°ca BTDC]
KI experimental
KI simulated (Sileghem)
KI simulated (Bougrine)

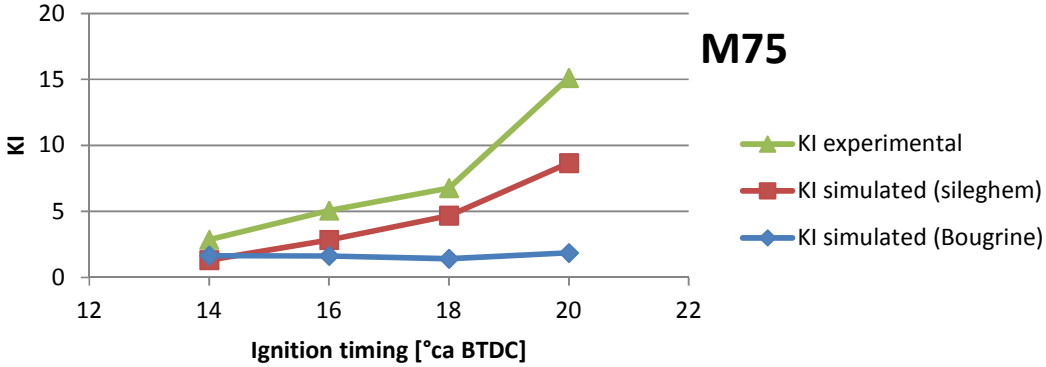
M75
KI
20
15
10
5
0
12
14
16
18
20
22
Ignition timing [°ca BTDC]
KI experimental
KI simulated (sileghem)
KI simulated (Bougrine)

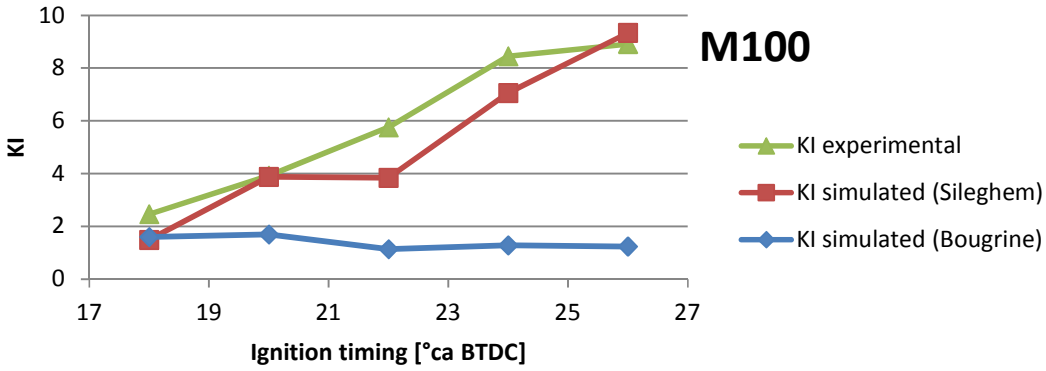
M100
KI
10
8
6
4
2
0
17
19
21
23
25
27
Ignition timing [°ca BTDC]
KI experimental
KI simulated (Sileghem)
KI simulated (Bougrine)

Figure 11 – Measured and simulated knock intensity for stoichiometric mixtures.

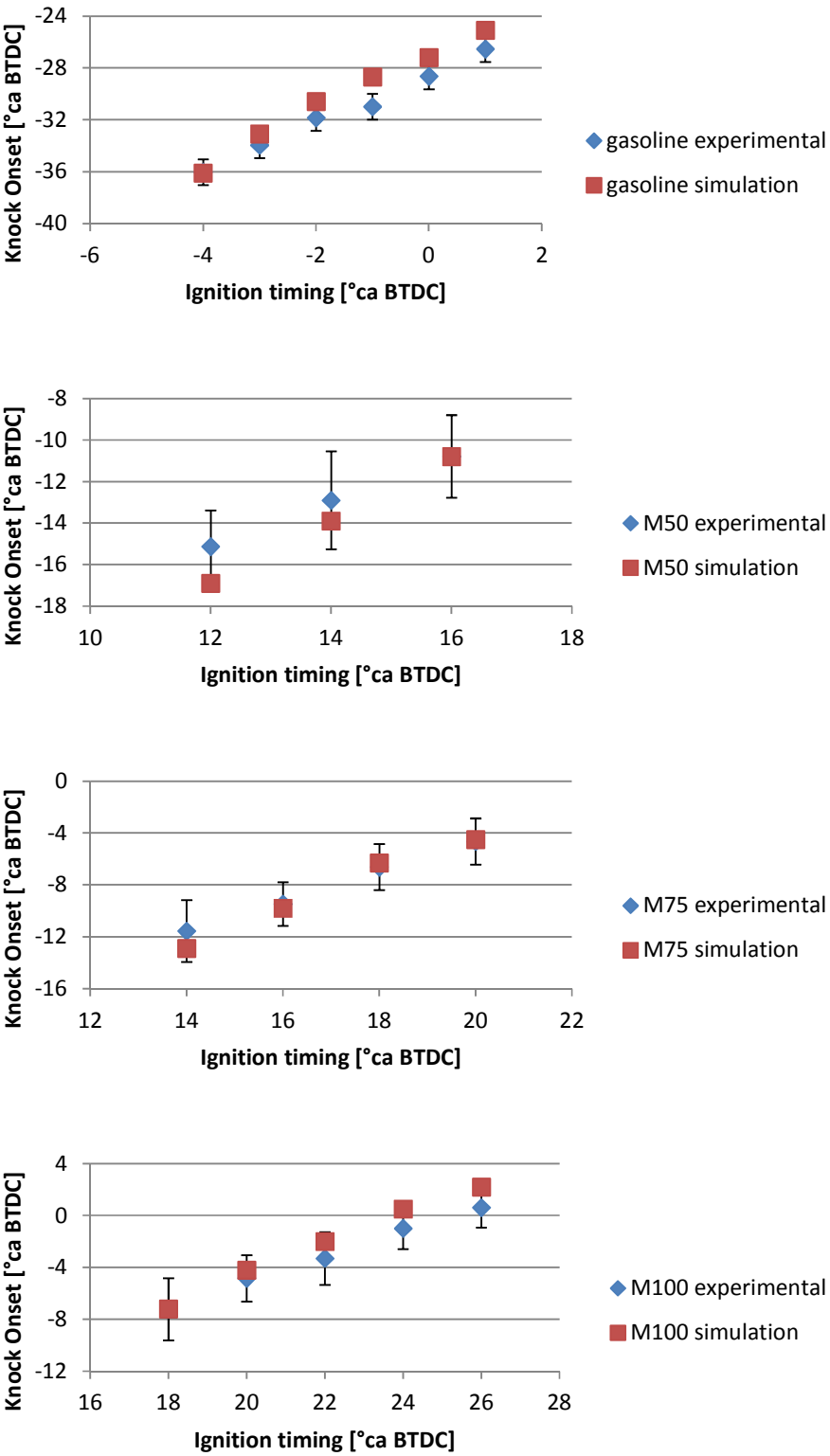

Figure 12 - Knock Onset stoichiometric mixtures

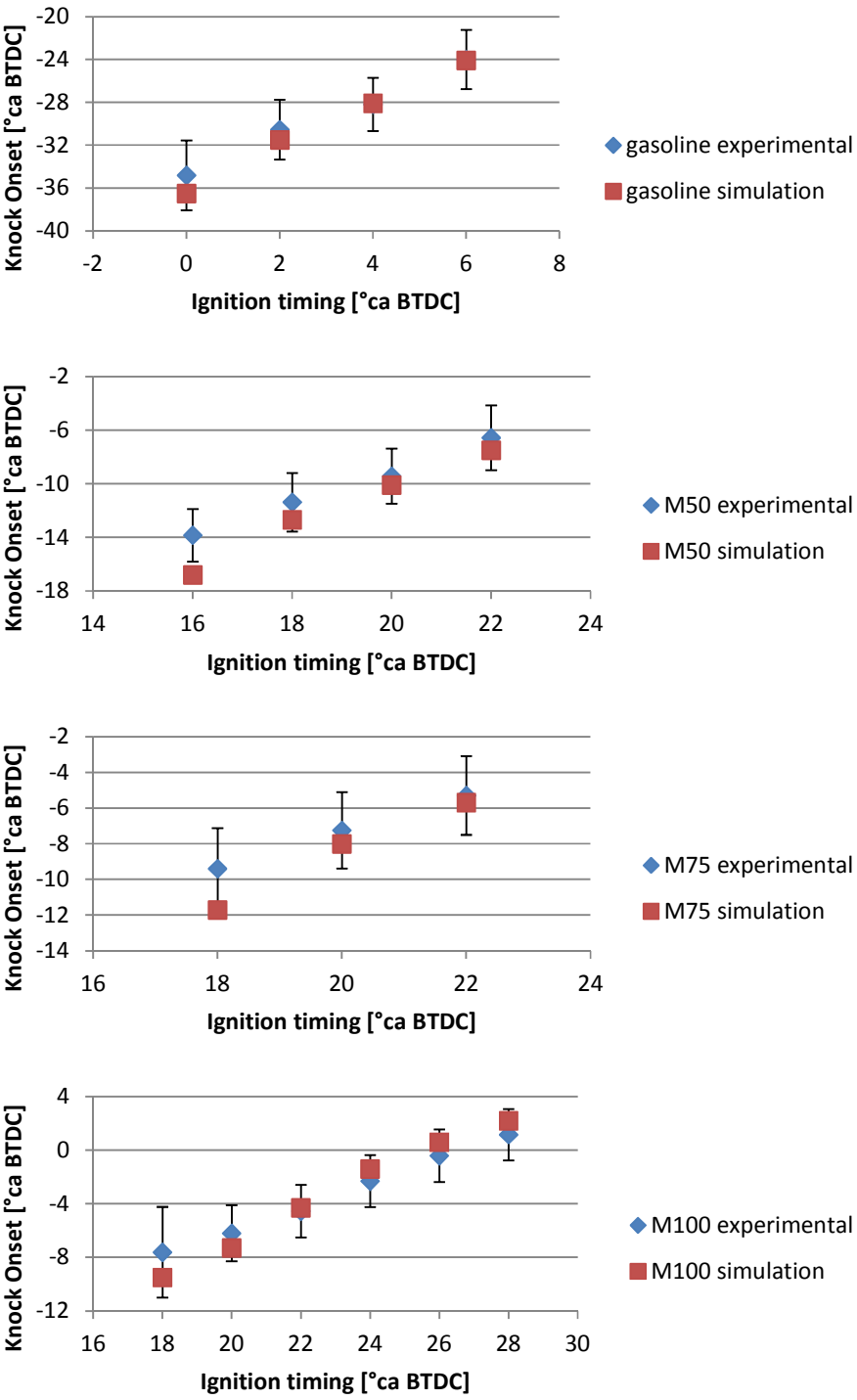

Figure 13 - Knock Onset lean mixtures

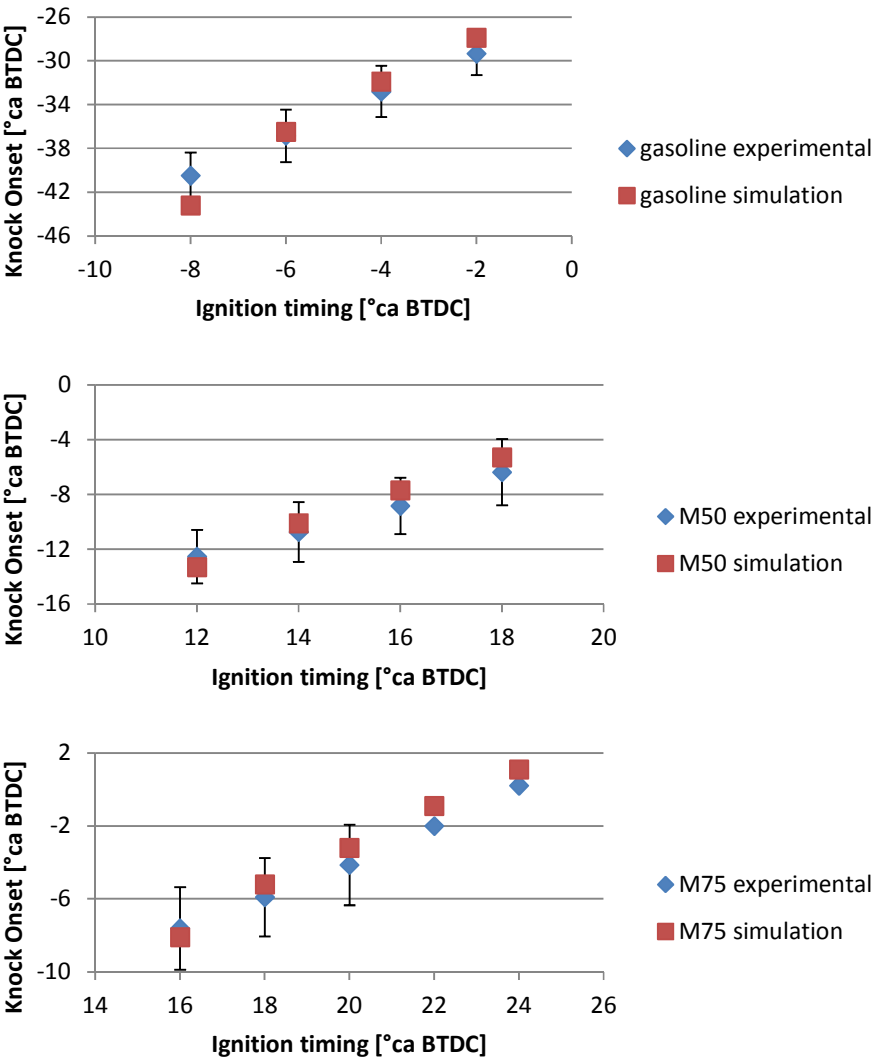

Figure 14 - Knock Onset rich mixtures

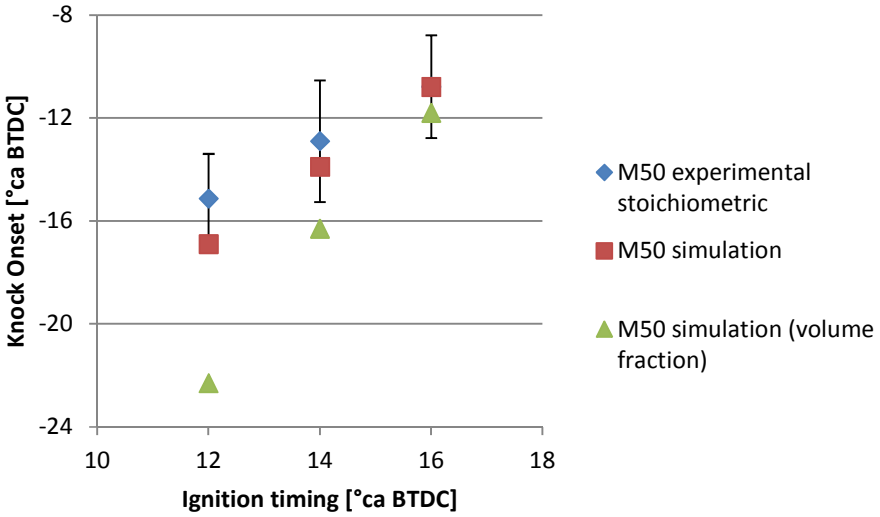
-8
-12
-16
-20
-24
Knock Onset [°ca BTDC]
10
12
14
16
18
Ignition timing [°ca BTDC]
M50 experimental stoichiometric
M50 simulation
M50 simulation (volume fraction)

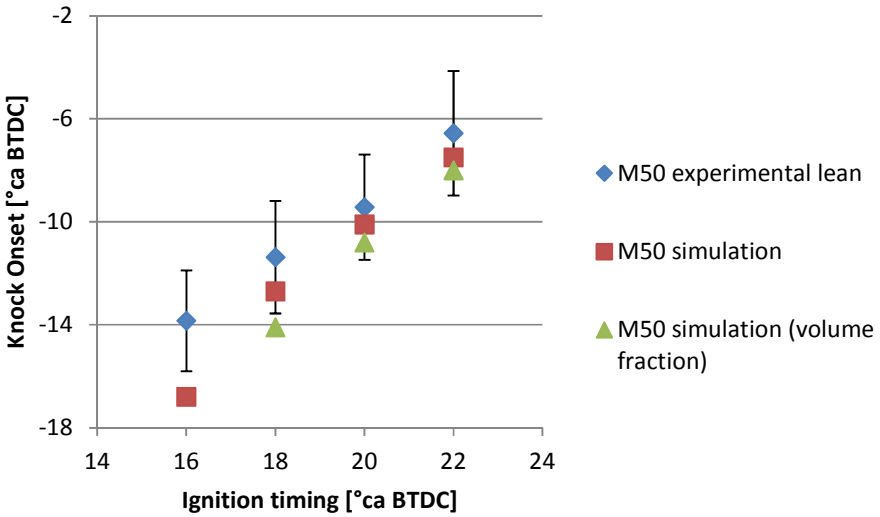
-2
-6
-10
-14
-18
Knock Onset [°ca BTDC]
14
16
18
20
22
24
Ignition timing [°ca BTDC]
M50 experimental lean
M50 simulation
M50 simulation (volume fraction)

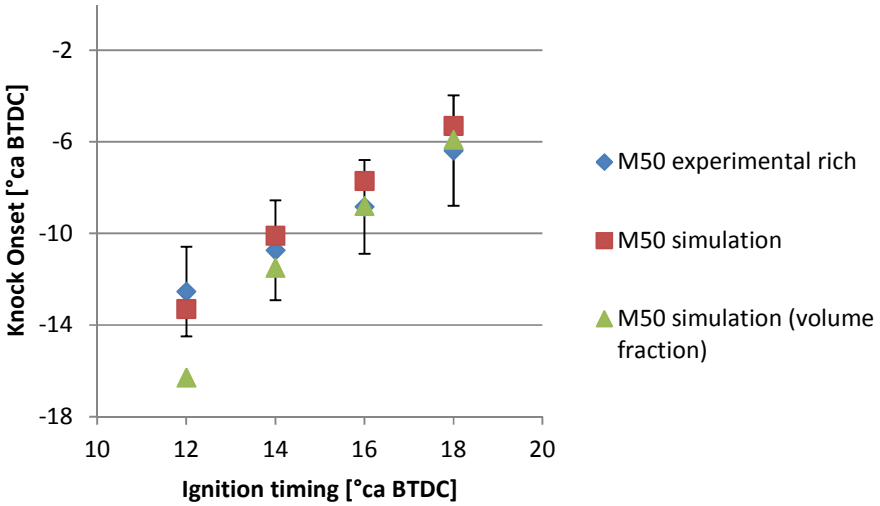
-2
-6
-10
-14
-18
Knock Onset [°ca BTDC]
10
12
14
16
18
20
Ignition timing [°ca BTDC]
M50 experimental rich
M50 simulation
M50 simulation (volume fraction)

Figure 15 – Knock Onset: Comparison between the energy fraction mixing rule with logarithmic value and volume fraction mixing rule with real values.